Inorganic Chemistry

Article

pubs.acs.org/IC

Three-Coordinate Nickel(II) and Nickel(I) Thiolate Complexes Based on the β-Diketiminate Ligand System

Bettina Horn, Christian Limberg,* Christian Herwig, and Beatrice Braun

Humboldt-Universität zu Berlin, Institut für Chemie, Brook-Taylor-Str. 2, 12489 Berlin, Germany

Supporting Information

ABSTRACT: Mononuclear nickel(II) thiolate complexes [L^{tBu}Ni(SEt)] (**1**) and [L^{tBu}Ni(aet)] (**2**, aet = $^{-}$S(CH$_2$)$_2$NH$_2$) (L^{tBu} = [HC(C(^{t}Bu)-NC$_6$H$_3$(^{i}Pr)$_2$)$_2$]$^-$), supported by a bulky nacnac ligand, were synthesized by treatment of the nickel(II) bromide precursor [L^{tBu}Ni(Br)] (**I**) with the potassium salts of ethanethiol and cysteamine, respectively. The nickel atom in **1** features a planar T-shaped environment, while the Ni ion within **2** shows a distorted square planar coordination geometry, as the aminoethanethiolate (aet) is coordinated as a chelating ligand. In **2** the β-diketiminate ligand binds in a rarely observed κ^2C,N coordination mode. Reduction of complex **1** or its benzenethiolate analogue [L^{tBu}Ni(SPh)] (**II**) by KC$_8$ resulted in the formation of dinuclear Ni^I thiolates (K·OEt$_2$)(K)[L^{tBu}Ni(SEt)]$_2$ (**3**) and (K·OEt$_2$)$_2$[L^{tBu}Ni(SPh)]$_2$ (**4**), respectively. In these compounds [L^{tBu}Ni-(SR)]$^-$ units are held together by potassium cations produced in the reduction process. All compounds mentioned were structurally characterized by single-crystal X-ray crystallography.

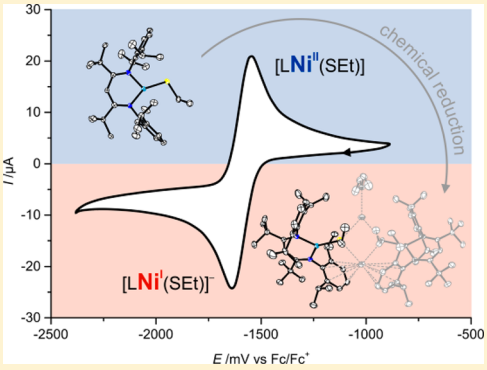

INTRODUCTION

The functions of enzymes, such as the [NiFe] carbon monoxide dehydrogenases (CODHs) that catalyze the interconversion of CO and CO_2 or the acetyl coenzyme A synthase (ACS), mediating the conversion of CO and coenzyme A to acetyl coenzyme A, are based on nickel centers ligated by cysteinate ligands.[1] As the ACS needs CO as the substrate, it occurs combined with a CODH subunit, which is called C-cluster, while the active site of the ACS is denoted as the A-cluster. Both are depicted in Figure 1. The C-cluster of well-characterized *Moorella thermoacetica* CODH/ACS$_{Mt}$ features a Ni^{II} ion, which is bound by three S ligands in a planar T-shaped coordination mode, and a "unique iron atom" (Fe$_u$) in close proximity;[2] in the first coordination sphere Fe$_u$ binds a histidine, a cysteine, and a μ_3-sulfide ligand plus a fourth light atom, supposed to be a H_2O/OH^- ligand, which is also near to the Ni ion.[3−7] The active state of the ACS contains a cysteine-ligated nickel ion (proximal to a Fe_4S_4 cluster), which according to the "paramagnetic proposal" is in the oxidation state +I prior to substrate binding.[8]

The coordination environments of the Ni centers within the C-cluster (CODH) and the ACS active site (A-cluster) have stimulated attempts to prepare synthetic structural model compounds for these metalloproteins, employing thiolates to mimic cysteinates,[7,9] and it is of particular interest to synthesize and investigate low-coordinate model compounds with reduced nickel centers exhibiting sulfur-based donors in its coordination spheres. In this work, we present the syntheses of three-coordinate nickel(II) complexes featuring a bidentate β-diketiminate ligand

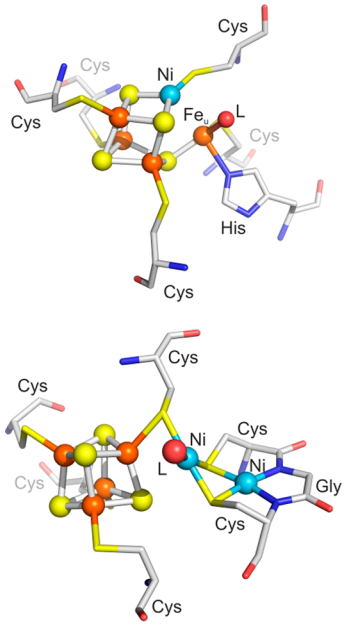

Figure 1. Ball-and-stick drawing of the C-cluster (top, CODH/ACS$_{Mt}$, PDB code: 3I01) and the A-cluster (bottom, ACS$_{Ch}$, PDB code: 1RU3).

("nacnac") system and one thiolate ligand and the investigation of their reduction.

Received: March 25, 2014
Published: June 10, 2014

   dx.doi.org/10.1021/ic500698v | Inorg. Chem. 2014, 53, 6867−6874

RESULTS AND DISCUSSION

Mononuclear Three-Coordinate Nickel(II) Thiolate Complexes. As the Ni^{II} ion in $[L^{tBu}Ni(Br)]$ (**I**) is already three-coordinated,[10,11] **I** appeared an ideal starting material for the synthesis of a variety of low-coordinate Ni complexes (L^{tBu} = $[HC(C(^tBu)NC_6H_3(^iPr)_2)_2]^-$). Recently, we communicated the synthesis of a nickel thiolate $[L^{tBu}Ni(SPh)]$ (**II**) with a Ni^{II} ion ligated by the N atoms of a bidentate β-diketiminate ("nacnac") ligand system and one S atom of a benzenethiolate anion in a T-shape coordination mode by a salt metathesis reaction involving **I** and 1 equiv of KSPh in tetrahydrofuran (THF).[12,13] Following the same procedure, but utilizing KSEt as the thiolate source, $[L^{tBu}Ni(SEt)]$ (**1**, Scheme 1) could be accessed. Complex **1** was isolated as a deep purple solid in 88% yield.

Scheme 1. Synthesis of the Nickel(II) Thiolate Compounds II,[12] 1, and 2

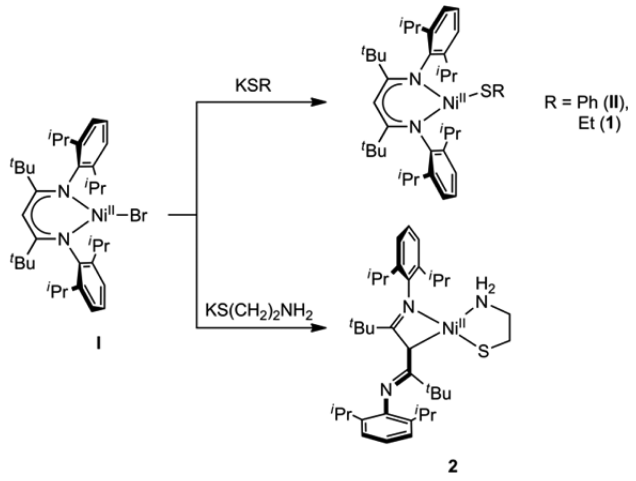

Single crystals suitable for X-ray diffraction analysis were obtained by cooling a hexane solution of **1** to −30 °C. They contain two independent molecules of $[L^{tBu}Ni(SEt)]$ (**1**) in the asymmetric unit, which differ in the conformation of the thiolate ligand. The molecular structure of one of these molecules is displayed in Figure 2. In the solid-state structure of **1** the coordination sphere of the three-coordinated Ni^{II} center can be described best as T-shaped planar (N2−Ni1−N1 96.06(10)° [96.24(9)°], N1−Ni1−S1 115.87(7)° [116.09(7)°], N2−Ni1−S1 148.03(7)° [147.65(7)°]; sum of angles 359.96(14)° [359.98(13)°]). The Ni−S distance of 2.1506(8) Å [2.1512(8) Å] is comparable to the value reported for the benzenethiolate analogue **II** (Table 1).

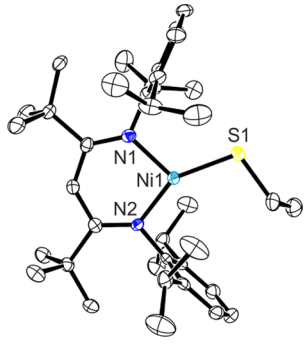

Figure 2. Molecular structure of one of two independent molecules of $[L^{tBu}Ni(SEt)]$ (**1**) in the asymmetric unit. Thermal ellipsoids are shown at 50% probability. All hydrogen atoms are omitted for clarity. Selected bond lengths and angles are summarized in Table 1.

Table 1. Selected Bond Lengths and Angles for the Nickel(II) Thiolate Complexes II and 1

bond (Å)/angle (deg)	II[12]	1[a]
Ni1−N1	1.9288(18)	1.921(2) [1.921(2)]
Ni1−N2	1.8658(19)	1.866(2) [1.876(2)]
Ni1−S1	2.1728(7)	2.1506(8) [2.1512(8)]
N2−Ni1−N1	96.37(7)	96.06(10) [96.24(9)]
N1−Ni1−S1	110.39(6)	115.87(7) [116.09(7)]
N2−Ni1−S1	153.08(6)	148.03(7) [147.65(7)]

[a]The values in square brackets correspond to the second independent molecule of **1**.

Solutions of complex **1** were found to be paramagnetic, exhibiting a solution magnetic moment of μ_{eff} = 2.67 μ_B at room temperature (r.t.) (Evans' method,[14] C_6D_6), which is consistent with the expectations for a high-spin Ni^{II} ion (S = 1, $\mu_{s.o.}$ = 2.83 μ_B). Accordingly, the ^1H NMR spectrum of **1** dissolved in C_6D_6 shows paramagnetically shifted signals corresponding to the protons of the nacnac ligand over a range from 50 to −200 ppm.[15] The electronic spectra of diethyl ether solutions of **II** and **1** are dominated by intense absorptions between 250 and 400 nm (**II**: ε_{max} = 13 mM^{-1} cm^{-1}, **1**: ε_{max} = 14 mM^{-1} cm^{-1}). Additionally, **II** and **1** exhibit two broad absorptions between 500 and 900 nm (ε_{max} = 2 mM^{-1} cm^{-1}), respectively. Density functional calculations (B3LYP Def2-SVP/TZVPD, see Supporting Information) confirm a triplet ground state with two unpaired electrons at the Ni atom (with T-shaped planar coordination) for both **II** and **1**.

Cyclic Voltammetry. The redox properties of the nickel(II) thiolates **II** and **1** were probed by cyclic voltammetry (CV) in THF with 0.1 M NBu_4PF_6 as electrolyte. The voltammograms of **II** and **1** (Figure 3) exhibit a reversible reduction wave at a low potential of −1.40 V (ΔE_p = 76 mV, scan rate 50 mV/s) and −1.60 V (ΔE_p = 81 mV, scan rate 50 mV/s) versus Fc/Fc^+, respectively, attributable to a Ni^{II}/Ni^{I} redox couple. Additionally, an irreversible oxidation can be observed at a higher potential of

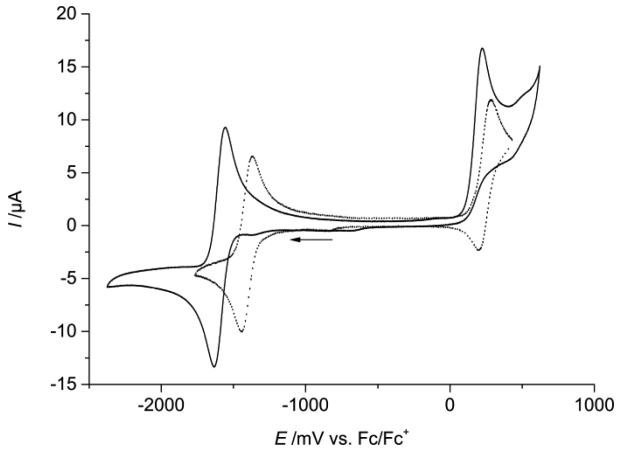

Figure 3. Cyclic voltammograms recorded for THF solutions containing **II** or **1** (1 mM) and NBu_4PF_6 (0.1 M). Full scan of **II** (····) and **1** (—) at 50 mV/s.

dx.doi.org/10.1021/ic500698v | Inorg. Chem. 2014, 53, 6867−6874

0.24 V for **1**, which becomes almost quasi-reversible at increasing scan rates (ΔE_p = 126 mV, scan rate 3158 mV/s, Figure S1, see Supporting Information). By contrast **II** shows quasi-reversible oxidation at a potential of 0.24 V (ΔE_p = 86 mV, scan rate 50 mV/s) even at low scan rates. The events observed at positive potential can be attributed to either a Ni^{II}/Ni^{III} couple or a ligand-based one-electron oxidation of the sulfur ligand leading to a thiyl radical. In the case of **II** the positive charge might get stabilized by the aromatic residue of the SPh ligand.

Reaction of Nickel(II) Thiolate Complexes II and 1 with CO. Although nickel(II) carbonyl units in sulfur-rich environments have been identified in several nickel-containing enzymes, such as CO dehydrogenases, synthetic model compounds are rather rare.[16] Therefore, hexane solutions of the thiolate complexes **II** and **1** were exposed to an atmosphere of CO and stirred for 6 h at r.t. However, after removal of the solvent mainly the corresponding thiolate compounds **II** and **1**, respectively, were isolated unchanged as evidenced by ^{1}H NMR spectroscopy. Additionally in both attempts the formation of traces of a Ni^I CO complex $[L^{tBu}Ni(CO)]$[17,18] was proved by IR spectroscopy through its characteristic absorption band (~2015 cm^{-1}) corresponding to the C−O stretching mode. Further evidence came from electron paramagnetic resonance (EPR) spectroscopy: solutions of the thiolates after CO treatment exhibited the characteristic rhombic signal caused by $[L^{tBu}Ni(CO)]$[18] (Figure S2, see Supporting Information). The thiolate ligands probably get oxidized in the presence of added CO, whereas the nickel(II) centers are reduced to nickel(I) yielding $[L^{tBu}Ni(CO)]$ through CO/RS· ligand substitution.[19] Interestingly, no reaction could be detected after treatment of $[L^{tBu}Ni(Br)]$ (**I**) with CO for 1 d.

A Nickel(II) Aminoethanethiolate Complex. Beside the more basic thiolates used in the syntheses of **II** and **1**, the introduction of ligands that can mimic the electronic and structural character of cysteinate more closely was also attempted to further approach the situation of the Ni center in the active site of CODH. With this aim we tried to deprotonate L-cysteine ethyl ester hydrochloride by different bases followed by treatment with 1 equiv of $[L^{tBu}Ni(Br)]$ (**I**). However, these reactions either yielded in decomposition products or the starting material was isolated back. By contrast, reaction of **I** with the potassium salt of cysteamine (see Scheme 1) in THF as the solvent led to the isolation of a red solid, after workup. After redissolution of the red residue in diethyl ether, single crystals suitable for X-ray diffraction were grown by fast evaporation of the solvent. The molecular structure of the reaction product $[L^{tBu}Ni(aet)]$ (**2**, aet = 2-aminoethanethiolate) is shown in Figure 4.

The Ni^{II} ion in **2** is coordinated in a distorted square planar fashion by bidentate *N,S*-aminoethanethiolate and nacnac ligands. The binding of the latter at the Ni center occurs not in the usual fashion via the two N donor functions but through interactions with the central carbon atom (C4) and one nitrogen atom (N2). The N2−C3 and N3−C5 bonds of 1.293(2) and 1.279(2) Å are slightly shorter than those found in other β-diketiminate nickel(II) compounds ($\mathbf{II}_{Ø}$: 1.34 Å, $\mathbf{1}_{Ø}$: 1.33 Å), whereas the C3−C4 and C4−C5 bond lengths of 1.502(2) and 1.492(2) Å are significantly longer than usual ($\mathbf{II}_{Ø}$: 1.40 Å, $\mathbf{1}_{Ø}$: 1.40 Å), indicating a diimine arrangement of the ligand. Hence, the negative charge of the ligand appears to be no longer delocalized over the ligand backbone but localized at the C4 atom, which thus binds as a carbanion. Both the Ni1−N2 and Ni1−S1 distances of 1.8947(14) and 2.1603(5) Å are similar to those found in **II** and **1**. A κ^2*C,N* coordination mode of a nacnac ligand at a metal center as in **2** has been found so far only in a small number of compounds including $[L^{Me}Pd(acac)]$[20] and $[L^{Me}GeCl_3]$[21] (L = $[HC(C(Me)NC_6H_3(^iPr)_2)_2]^-$). Although **2** is somewhat unstable in solution—an insoluble precipitate is formed upon storage[22]—it could be characterized by ^{1}H NMR spectroscopy. The spectrum (C_6D_6, r.t.) shows that **2** is diamagnetic and reveals resonances at δ(H) 7.28 and 2.34 ppm, which correspond to the two methylene groups of the thiolate ($S(CH_2)_2NH_2$), while the amine group gives rise to a signal at δ(H) −3.09 ppm. It is noteworthy that in solution the protons of the two imine-based parts of the nacnac ligand ($C(^tBu)$=$N-C_6H_3(^iPr)_2$) seem to be equivalent, as they result in only one set of signals. This observation suggests a fast exchange of the coordinated and noncoordinated imine functions. A signal for the proton bound to the central C4 atom of the nacnac backbone could not be detected at r.t. perhaps due to masking. Upon cooling a THF-d_8 solution of **2** (in a variable-temperature NMR experiment), a number of signals experience significant shifts (Figure S3, see Supporting Information), and at −40 °C the resonance for the central CH unit became visible at δ(H) 3.9 ppm, shifting further to δ(H) 4.8 ppm at −80 °C. The shifting of signals with temperature may be due to a population/depopulation of an excited triplet state[23] of **2** or due to a coexisting isomer with a significantly different structure in solution.

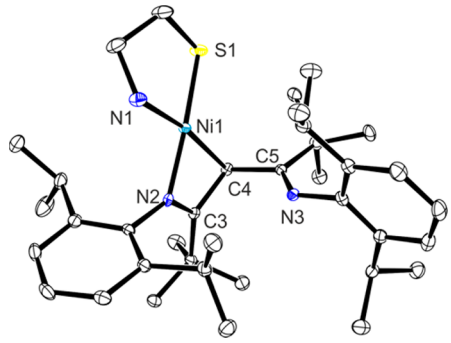

Figure 4. Molecular structure of $[L^{tBu}Ni(aet)]$ (**2**). Thermal ellipsoids are shown at 50% probability. All hydrogen atoms are omitted for clarity. Selected bond lengths (Å) and angles (deg): Ni1−N1 1.9593(14), Ni1−N2 1.8947(14), Ni1−C4 2.0097(16), Ni1−S1 2.1603(5), N2−C3 1.293(2), C3−C4 1.502(2), C4−C5 1.492(2), C5−N3 1.279(2), N2−Ni1−N1 98.52(6), N2−Ni1−C4 69.86(6), N1−Ni1−S1 88.81(4), C4−Ni1−S1 103.31(5).

Reaction of 2 with O_2. Complex **2** exhibits a pronounced sensitivity toward O_2, which thus was inspected more closely. The UV−vis spectrum of **2** at r.t. dissolved in diethyl ether exhibits two intense absorption features at 299 nm (ε = 16 mM^{-1} cm^{-1}) and 331 nm (ε = 12 mM^{-1} cm^{-1}) and one additional broad absorption band at 414 nm (ε = 4 mM^{-1} cm^{-1}). In the course of the reaction with O_2 these bands decrease (Figure S4, see Supporting Information). The fact that no new band evolved may indicate the cleavage of the Ni−S bond[24] or even the total decomposition of complex **2**. The oxygenated solution was further analyzed by mass spectrometry, and the results hinted *inter alia* to the formation of a monooxygenated product, which was supported by isotope labeling using $^{18}O_2$ (Figure S5, see Supporting Information). These results suggest an oxygenation of the sulfur donor moiety yielding in a sulfenate complex. To further test this assumption the product was investigated by IR spectroscopy. However, characteristic S=O stretching vibration bands (in the region of 900−1200 cm^{-1})[25] for oxygenated species of **2** could not be detected, and the results of additional ^{1}H NMR

dx.doi.org/10.1021/ic500698v | Inorg. Chem. 2014, 53, 6867−6874

spectroscopic measurements pointed to the formation of a product mixture.

Dinuclear Nickel(I) Thiolate Complexes. Structurally characterized synthetic nickel(I) thiolate complexes are extremely scarce. We recently reported an example where an expanded β-diketiminate ligand system with two binding pockets was utilized as a ligand for a $Ni^{I}-(\mu\text{-SR})-Ni^{I}$ unit with strongly antiferromagnetically coupled Ni^{I} ions.[26] Tatsumi et al. described the syntheses of $[(PPh_3)Ni(SDmp)]$ (Dmp = 2,6-dimesitylphenyl) and $[(PPh_3)Ni(\mu\text{-SR})]_2$ (R = 2,4,6-triisopropylphenyl or 1-adamantyl) via reactions of a Ni^{I} amide precursor with the corresponding thiols.[16c] A similar dinuclear Ni^{I} complex $[(P^{i}Pr_3)Ni(\mu\text{-SPh})]_2$ with bridging thiolate ligands could be isolated by Johnson and co-workers after slow dimerization of $[(P^{i}Pr_3)_2Ni(SPh)(H)]$ accompanied by loss of H_2 and two phosphine ligands; an alternative synthetic route utilized a salt metathesis reaction of PhSLi with $[(P^{i}Pr_3)_2Ni(Cl)]$.[27] Recently, Duboc et al. described the synthesis of a mononuclear Ni^{I} diamine aliphatic dithiolate complex through bulk electrolyses, which was claimed as the first example of a representative with a purely aliphatic thiolate N_2S_2 environment.[28]

This background and the fact that the CV measurements on complexes **II** and **1** indicated that they can be reduced under electrochemical conditions and remain stable after reduction (→ reversibility) stimulated attempts to achieve reduction chemically. Indeed, $[L^{tBu}Ni(SEt)]$ (**1**) reacts with 1 equiv of potassium graphite yielding a nickel(I) product.[29] The product was crystallized from diethyl ether at −30 °C, and a single-crystal X-ray analysis identified it as the dinuclear compound $(K{\cdot}OEt_2)(K)[L^{tBu}Ni(SEt)]_2$ (**3**, Scheme 2).

Scheme 2. Synthesis of 3 and 4 by Reaction of $[L^{tBu}Ni(SR)]$ (Path A: R = Et (1), Path B: R = Ph (II)) with KC_8 in Hexane, Followed by Workup with Diethyl Ether

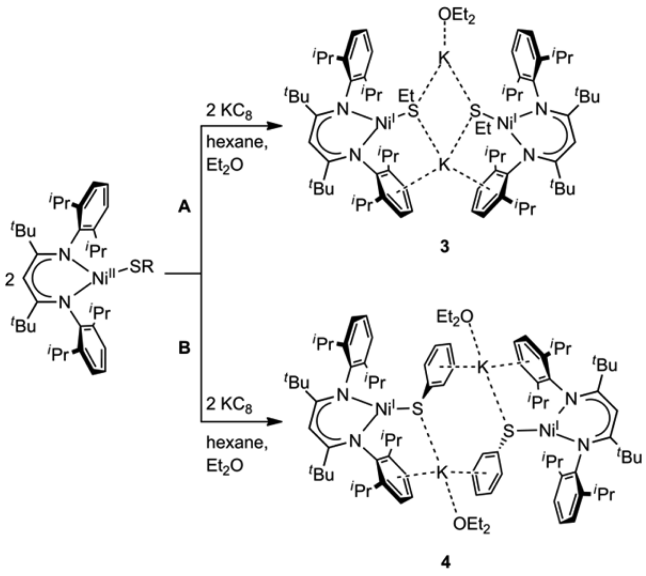

In **3** two crystallographically equivalent $[L^{tBu}Ni^{I}(SEt)]^{-}$ moieties are held together (Ni1···Ni1′ 7.8692(6) Å) by two K^{+} ions (Figure 5) produced in the reduction process, and these cations interact with the S atoms of the thiolate ligand (S···K 3.0683(7)−3.1023(7) Å). In addition, K2 interacts with the aryl rings of the diketiminate (Ar···K2 3.0033(4) Å), whereas the

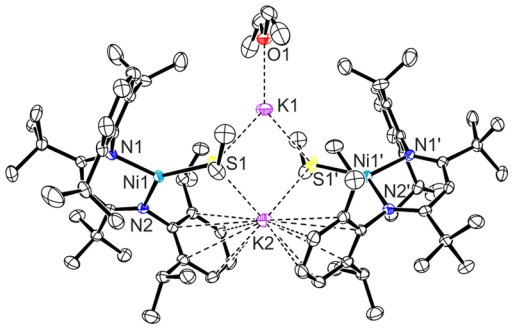

Figure 5. Molecular structure of $(K{\cdot}OEt_2)(K)[L^{tBu}Ni(SEt)]_2$ (**3**). Thermal ellipsoids are shown at 50% probability. All hydrogen atoms are omitted for clarity. Selected bond lengths and angles are summarized in Table 2.

Table 2. Selected Bond Lengths and Angles for the Nickel(I) Thiolate Complexes 3 and 4

bond (Å)/angle (deg)	3	4
Ni1−N1	1.9156(15)	1.9048(9)
Ni1−N2	1.9109(16)	1.9243(9)
Ni1−S1	2.1986(6)	2.2471(3)
K1···S1	3.0683(7) [3.1023(7)][b]	3.3428(4)
K1···S1′	3.0684(7) [3.1023(7)][b]	3.1676(4)
K1···O1	2.613(2)	2.7696(9)
N1−Ni1−N2	97.47(6)	98.04(4)
N1−Ni1−S1	129.56(5)	144.49(3)
N2−Ni1−S1	132.85(8)	117.24(3)

[b]The values in square brackets correspond to the K2···S1 and K2···S1′ distances, respectively.

second potassium ion (K1) is associated with one solvent molecule (O1···K1 2.613(2) Å). The trigonal planar coordination around the nickel center found for the mononuclear precursor **1** is maintained in **3** (N−Ni−N 97.47(6)°, N−Ni−S 129.56(5)° and 132.85(8)°, sum of angles 359.88(11)°). However, in contrast to the distorted T-shape ligand environment of the Ni^{II} ion in **1**, the solid-state structure of **3** contains the Ni ions in Y-shaped coordination geometries, which is reflected by two similar N−Ni−S angles per Ni center. The Ni1−S1 bond length of 2.1986(6) Å is marginally longer (**1**: 2.1506(8) [2.1512(8)] Å), whereas the Ni−N distances of 1.9156(15) and 1.9109(16) Å are comparable to the corresponding values found in the nickel(II) thiolate complex **1** (Table 1).

To determine whether the Y-geometry arises from electronic or steric effects, we investigated the structure of one of the $[L^{tBu}Ni(SEt)]^{-}$ moieties found in **3** using density functional theory (DFT) (B3LYP Def2-SVP/TZVPD). Geometry optimization of a $[L^{tBu}Ni^{I}(SEt)]^{-}$ fragment cut out of the structure of **3** as determined by X-ray analysis gives a doublet ground state with Y coordination. The optimized geometry shows fair agreement with the metric data of the $[L^{tBu}Ni(SEt)]^{-}$ fragments in **3**, and these results therefore suggest that electronic reasons are responsible for the preference of a Y-shaped geometry in the Ni^{I} complex.

Reduction of $[L^{tBu}Ni(SEt)]$ (**1**) by one electron suggests an oxidation state of +I for the Ni ions in the dimeric product **3**, and the spin-only value for two uncoupled Ni^{I} ions ($S_1 = S_2 = 1/2$) amounts to 2.45 μ_B. Magnetic measurements at r.t. showed a slightly higher value of $\mu_{eff} \approx 3.0\ \mu_B$ in solution as well as in the solid state for **3**. Additional evidence for the existence of Ni^{I} ions

dx.doi.org/10.1021/ic500698v | Inorg. Chem. 2014, 53, 6867−6874

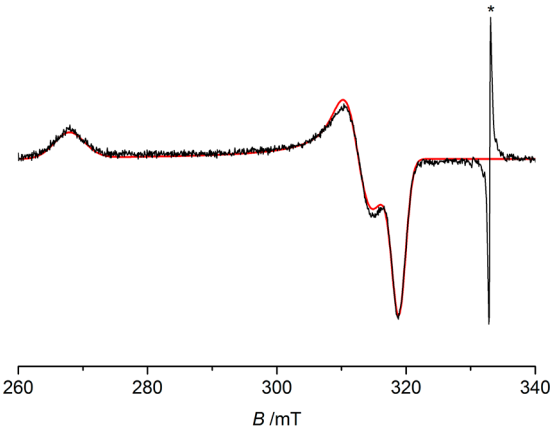

Figure 6. EPR spectrum of **3** dissolved in diethyl ether at 77 K. Black line: experimental spectrum with MgO/Cr^{3+} (*) as an internal standard, red line: simulation. The g values were determined to be $g_x = 2.461$, $g_y = 2.110$, and $g_z = 2.068$ (spectrometer frequency: 9.22 GHz).

in **3** was provided by an EPR spectrum recorded for a diethyl ether solution at 77 K (Figure 6), which exhibited a rhombic signal ($g_x = 2.461$, $g_y = 2.110$, $g_z = 2.068$) that is typical for nacnac Ni^I complexes ($S = 1/2$).[11,30]

The results of analogous reduction studies with **II** showed that the steric demand of the thiolate ligand does not affect the formation of a Ni^I dimer: treatment of **II** with 1 equiv of KC_8 in hexane and storage of a diethyl ether solution of the product at r.t. afforded red crystals of $(K{\cdot}OEt_2)_2[L^{tBu}Ni(SPh)]_2$ (**4**) (Scheme 2), as confirmed by single-crystal X-ray diffraction analysis (Figure 7).

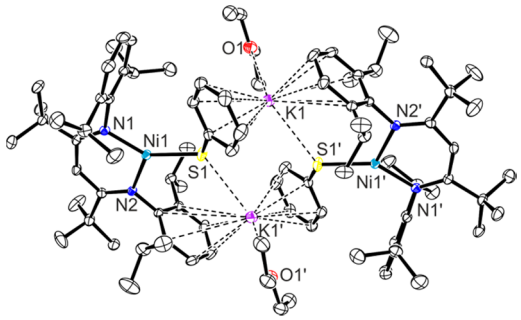

Figure 7. Molecular structure of $(K{\cdot}OEt_2)_2[L^{tBu}Ni(SPh)]_2$ (**4**). Thermal ellipsoids are shown at 50% probability. All hydrogen atoms are omitted for clarity. Selected bond lengths and angles are summarized in Table 2.

As with **3**, complex **4** is composed of two crystallographically equivalent $[L^{tBu}Ni(SPh)]^-$ moieties held together by K^+ ions. However, while in **3** linkage by the K^+ cations occurs through electrostatic interactions involving nacnac aryl rings and the thiolate S atoms, in **4** the phenyl residues of the thiolate ligands rather than their S atoms (showing comparatively large distances to the K^+ ions, see Table 2), are involved: each K^+ ion interacts with one aryl ring of the nacnac ligand system ($Ar_{nacnac}\cdots$K 3.0777(3) Å) and one phenyl ring of the benzenethiolate ($Ar_{SPh}\cdots$K 2.9825(3) Å) as well as with one Et_2O molecule (O1···K1 2.7696(9) Å). The Ni1−S1 bond length of 2.2471(3) Å is longer compared to the corresponding bonds found in the nickel(II) thiolate complexes (**1** and **II**; 2.15−2.17 Å; Table 1). The increase of the Ni−S distance by ∼0.05 Å on going from ethanethiolate in nickel(I) complex **3** to benzenethiolate in **4** follows the same trend as observed for the mononuclear nickel(II) compounds **1** and **II**.

Obviously, due to both the more bulky thiolate ligands and the altered interactions of the K^+ ions the Ni···Ni distance is much larger in the solid-state structure of **4** (9.0041(4) Å) than it is in **3**. Notably, the Ni ions in **4** are in a coordination environment that can be described best as T-shaped (N−Ni−N 98.04(4)°, N−Ni−S 144.49(3)° and 117.24(3)°), which is in conflict with the Y-shaped geometry as found in the molecular structure of **3** and theoretically for a $[L^{tBu}Ni(SEt)]^-$ model (see above). In fact, DFT predicts a Y-shape also for $[L^{tBu}Ni(SPh)]^-$, so that the T-shape found will have its origin in restrictions caused by aggregation via the K^+ ions.

Interestingly, the solubilities found for **3** and **4** are complementary: while **3** is only sparingly soluble in hexane but dissolves well in Et_2O, **4** behaves the other way round. Magnetic measurements at r.t. for **4** found $\mu_{eff} = 2.79\ \mu_B$ (Evans' method,[14] C_6D_6, $\mu_{s.o.} = 2.45\ \mu_B$). The EPR spectrum recorded for a diethyl ether solution of **4** at 77 K (Figure S6, see Supporting Information) exhibited a rhombic signal ($g_x = 2.463$, $g_y = 2.108$, $g_z = 2.068$)[31] that is similar to the one recorded for the Y-coordinated Ni^I complex **3**, which suggests a similar Y-shaped structure in solution.

Complexes **3** and **4** represent novel examples of the still small family of structurally characterized nickel(I) thiolate complexes: to our knowledge these are the first dinuclear representatives, where the thiolates do not function as bridging ligands.

Treatment of 3 and 4 with CO. Exposure of a hexane suspension of **3** to an atmosphere of CO at r.t. immediately produced the mononuclear Ni^I carbonyl complex $[L^{tBu}Ni(CO)]$[17] as the major product (as evidenced by the ^1H NMR and IR spectrum of the crude product), accompanied by the formation of KSEt. The stability of the latter allows for the exchange of the thiolate ligands by CO. Upon treatment of a hexane solution of the benzenethiolate derivative **4** it reacts with CO in an analogous manner to give $[L^{tBu}Ni(CO)]$ and KSPh, as proved by IR and NMR spectroscopy.

■ CONCLUSION

Inspired by the 3-fold S-ligated nickel centers found in metalloenzymes such as the CODH or ACS, the introduction of thiolates into the coordination spheres of $[L^{tBu}Ni]^+$ moieties was investigated. Complex $[L^{tBu}Ni(SEt)]$ (**1**) could be accessed displaying a three-coordinate Ni center with a T-shaped environment. In an attempt to approach the electronic situation provided by a cysteinate ligand more closely aminoethanethiolate was employed as a ligand, too, which led to a nickel(II) complex with a distorted square planar ligand coordination geometry composed of a chelating $NH_2(CH_2)_2S^-$ unit and a diketiminate ligand in an unusual κ^2C,N coordination mode. The thiolate compounds did not exhibit a pronounced reactivity toward CO even though $[L^{tBu}Ni(CO)]$ was found in traces. Reduction of **1** and its benzenethiolate analogue by KC_8 led to rare examples of structurally characterized nickel(I) thiolate complexes, which may serve as models for intermediates in the catalytic cycle of the ACS.

■ EXPERIMENTAL SECTION

General Procedures. All manipulations were carried out in a glovebox or else by means of Schlenk-type techniques involving the use of a dry argon atmosphere. The ^1H and ^{13}C NMR spectra were recorded on a Bruker DPX 300 NMR spectrometer at r.t. (^1H: 300.1 MHz, ^{13}C: 75.5 MHz). ^1H and ^{13}C chemical shifts are reported in ppm and

dx.doi.org/10.1021/ic500698v | Inorg. Chem. 2014, 53, 6867−6874

were calibrated internally to the solvent signals (C_6D_6: δ_H 7.16 and δ_C 128.06 ppm, deuterated dimethyl sulfoxide (DMSO-d_6): δ_H 2.50 ppm). Solution magnetic susceptibilities were determined by the Evans' method[14] at r.t. with a Bruker DPX 300 (300.1 MHz) or AV 400 (400.1 MHz) NMR spectrometer. The samples were measured in C_6D_6 with 1% tetramethylsilane (TMS), together with a capillary tube that contained C_6D_6 with 1% TMS as an internal standard. The magnetic moment of the solid sample was determined by using a magnetic balance (Alfa) at r.t. Ultraviolet−visible (UV−vis) spectra were obtained on an Agilent 8453 UV−visible spectrophotometer using quartz cuvettes. Mass spectra (electrospray ionization) were recorded on an Agilent Technologies 6210 Time-of-Flight LC-MS instrument. Infrared (IR) spectra were recorded using solid samples prepared as KBr pellets with a Shimadzu FTIR-8400S-spectrometer. Microanalyses were performed on a HEKAtech Euro EA 3000 analyzer. EPR spectra were recorded at the X-band spectrometer ERS 300 (ZWG/Magnettech, Berlin/Adlershof) equipped with a fused quartz Dewar for measurements at liquid nitrogen temperature. The g factors were calculated with respect to a Cr^{3+}/MgO reference (g = 1.9796). CV was performed with a GAMRY Reference 600 potentiostat. The 3-electrode setup consisted of a 3 mm glassy carbon disc working, Radiometer M241Pt counter, and Pt wire pseudoreference electrodes. Electrochemical measurements were carried out at r.t. and under an argon atmosphere. At the end of each experiment a small amount of ferrocene was added to the respective solution, and all data were then referenced against the Fc/Fc^+ redox couple as an internal standard. Cyclic voltammograms were collected at scan rates of 50−3158 mV/s.

Materials. Solvents were dried employing an MBraun Solvent Purification System. [L^{tBu}Ni(Br)][32] (**I**) and [L^{tBu}Ni(SPh)][12] (**II**) were prepared according to literature procedures. To synthesize the potassium salts KSR (R = Et, $-(CH_2)_2NH_2$) the appropriate thiol was treated with a slight excess of KOMe (1.1 equiv) suspended in THF and stirred for 12 h. The resulting suspension was filtered, and the residue was dried in vacuum.

Synthesis of [L^{tBu}Ni(SEt)] (1). [L^{tBu}Ni(Br)] (**I**) (300 mg, 0.47 mmol) was dissolved in 20 mL of THF, KSEt (52 mg, 0.52 mmol, 1.1 equiv) was added, and the reaction mixture was stirred for 12 h. After filtration, the solvent was evaporated under vacuum, and the residue was extracted with hexane (20 mL). Filtration yielded a dark blue solution. The solvent was removed in vacuum to give **1** as a dark violet solid (256 mg, 0.41 mmol, 88%). ^{1}H NMR (C_6D_6, 300.1 MHz): δ = 48 (4H, Ar-*m***H**), 31 (4H, C**H**$(CH_3)_2$), 14 (3H, SCH_2CH_3), 10 (12H, $CH(CH_3)_2$), 8 (12H, $CH(CH_3)_2$), 4 (18H, $C(CH_3)_3$), −54 (2H, Ar-*p***H**), −201 (1H, **CH**$CC(CH_3)_3$) ppm; μ_{eff} (C_6D_6, 400.1 MHz) = 2.67 μ_B; UV−vis (Et_2O): λ_{max} (ε in mM^{-1} cm^{-1}) = 290 (sh, 12.5), 304 (sh, 13), 315 (14), 340 (sh, 9), 385 (sh, 2), 567 (2), 701 (2) nm; IR (KBr): $\tilde{\nu}$ = 3060 (m), 3050 (m), 3016 (m), 3003 (m), 2957 (vs), 2925 (s), 2866 (s), 1918 (w), 1854 (w), 1537 (m), 1508 (s), 1463 (m), 1442 (m), 1433 (m), 1381 (m), 1374 (m), 1352 (vs), 1317 (s), 1251 (m), 1221 (m), 1209 (m), 1196 (m), 1181 (m), 1153 (w), 1136 (m), 1098 (m), 1059 (w), 1053 (w), 1032 (w), 968 (m), 933 (m), 887 (w), 819 (m), 802 (m), 798 (m), 778 (s), 754 (m), 673 (w), 648 (w) cm^{-1}; elemental analysis (%) calcd for $C_{37}H_{58}N_2NiS$ (621.63 g mol^{-1}): C 71.49, H 9.40, N 4.51; found: C 71.62, H 9.50, N 4.20.

Synthesis of [L^{tBu}Ni(aet)] (2). [L^{tBu}Ni(Br)] (**I**) (150 mg, 0.23 mmol) was dissolved in 20 mL of THF, $KS(CH_2)_2NH_2$ (30 mg, 0.26 mmol, 1.1 equiv) was added, and the reaction mixture was stirred for 12 h. The suspension was filtered, and the solvent was evaporated under vacuum. The resulting residue was washed with hexane (5 mL) and dried in vacuum to give **2** as a red solid (90 mg, 0.14 mmol, 60%). ^{1}H NMR (C_6D_6, 300.1 MHz): δ = 7.72 (d, $^3J_{HH}$ = 7.6 Hz, 4H, Ar-*m***H**), 7.28 (br, 2H, $SCH_2CH_2NH_2$), 5.97 (t, $^3J_{HH}$ = 7.6 Hz, 2H, Ar-*p***H**), 4.90 (br, 4H, C**H**$(CH_3)_2$), 2.34 (br, 14H, $CH(CH_3)_2$ (12H) and $SCH_2CH_2NH_2$ (2H)), 1.50 (br, 12H, $CH(CH_3)_2$), 1.09 (s, 18H, $C(CH_3)_3$), −3.09 (br, 2H, $SCH_2CH_2NH_2$) ppm; ^{13}C NMR (C_6D_6, 75.5 MHz): δ = 158.8 (Ar-*o***C**), 145.0 (Ar-*i***C**), 132.0 (Ar-*p***C**), 119.2 (Ar-*m***C**), 30.8 ($C(CH_3)_3$), 30.4 ($CH(CH_3)_2$), 26.1 ($CH(CH_3)_2$), 25.1 (**C**H$(CH_3)_2$) ppm; UV−vis (Et_2O): λ_{max} (ε in mM^{-1} cm^{-1}) = 299 (16), 331 (12), 394 (sh, 3.5), 414 (4) nm; electrospray ionization mass spectrometry (ESI-MS) (250 V, pos): m/z = 636.3879 ([L^{tBu}Ni(aet)+H]$^+$, calcd: 636.3861), 658.3695 ([L^{tBu}Ni(aet)+Na]$^+$, calcd: 658.3681); IR (KBr): $\tilde{\nu}$ = 3312 (m), 3265 (w), 3249 (w), 3056 (m), 3050 (m), 2962 (vs), 2928 (s), 2903 (s), 2868 (s), 2835 (m), 1612 (s), 1603 (s), 1586 (s), 1512 (w), 1477 (s), 1461 (s), 1441 (m), 1429 (m), 1408 (s), 1396 (s), 1383 (m), 1364 (m), 1324 (s), 1252 (m), 1214 (m), 1189 (m), 1178 (m), 1160 (w), 1122 (m), 1091 (m), 1080 (m), 1061 (s), 1039 (m), 1028 (m), 999 (s), 960 (m), 936 (m), 889 (w), 877 (m), 865 (w), 850 (m), 820 (w), 800 (s), 770 (s), 760 (s), 689 (w) cm^{-1}; elemental analysis (%) calcd for $C_{37}H_{59}N_3NiS$ (636.64 g mol^{-1}): C 69.80, H 9.34, N 6.60; found: C 69.48, H 9.41, N 6.10.

Synthesis of (K·OEt_2)(K)[L^{tBu}Ni(SEt)]$_2$ (3). A dark blue hexane solution of [L^{tBu}Ni(SEt)] (**1**) (100 mg, 0.16 mmol) was treated with KC_8 (23 mg, 0.17 mmol, 1.1 equiv) and stirred for 12 h. All volatiles of the resulting red suspension were removed in vacuum. The residue was extracted with diethyl ether (10 mL). Removal of the solvent yielded **3** as a red solid, which was dried in vacuum (73 mg, 0.05 mmol, 65%). ^{1}H NMR (C_6D_6, 300.1 MHz): δ = 3.5 (br), −1.1 (br) ppm; μ_{eff} (solution, C_6D_6, 300.1 MHz) = 2.90 μ_B; μ_{eff} (solid, r.t.) = 3.08 μ_B, UV−vis (Et_2O): λ_{max} (ε in mM^{-1} cm^{-1}) = 285 (sh, 26), 315 (33), 387 (11), 450 (sh, 6), 550 (sh, 2), 700 (1) nm; IR (KBr): $\tilde{\nu}$ = 3052 (m), 3011 (m), 2958 (vs), 2905 (s), 2868 (s), 1904 (w), 1849 (w), 1618 (w), 1581 (w), 1532 (m), 1503 (s), 1463 (m), 1444 (m), 1425 (s), 1404 (vs), 1365 (s), 1324 (s), 1253 (m), 1219 (m), 1195 (m), 1184 (m), 1155 (m), 1096 (m), 1057 (w), 1040 (w), 1028 (m), 964 (w), 935 (m), 889 (m), 878 (m), 843 (w), 803 (m), 776 (m), 757 (m), 707 (w), 680 (w), 648 (w) cm^{-1}; elemental analysis (%) calcd for $C_{78}H_{126}K_2N_4Ni_2OS_2$ (1395.57 g mol^{-1}): C 67.13, H 9.10, N 4.01; found: C 66.92, H 9.00, N 4.09.

Synthesis of (K·OEt_2)$_2$[L^{tBu}NiSPh]$_2$ (4). A dark green hexane solution of [L^{tBu}Ni(SPh)] (**II**) (100 mg, 0.15 mmol) was treated with KC_8 (22 mg, 0.16 mmol, 1.1 equiv) and stirred for 12 h. The suspension was filtered, and the solvent was evaporated under vacuum. Crystallization from diethyl ether at −30 °C yielded red crystals of **4**, which were dried in vacuum (68 mg, 0.04 mmol, 58%). ^{1}H NMR (C_6D_6, 300.1 MHz): δ = 3.6 (br), −0.9 (br) ppm; μ_{eff} (solution, C_6D_6, 300.1 MHz, 21 °C) = 2.79 μ_B; UV−vis (Et_2O): λ_{max} (ε in mM^{-1} cm^{-1}) = 290 (sh, 33), 315 (41), 390 (sh, 10), 421 (sh, 9), 535 (sh, 2), 780 (1) nm; IR (KBr): $\tilde{\nu}$ = 3052 (w), 2958 (vs), 2927 (s), 2905 (s), 2868 (m), 1620 (w), 1575 (m), 1532 (m), 1502 (m), 1460 (m), 1444 (m), 1424 (m), 1402 (vs), 1365 (s), 1323 (s), 1253 (w), 1219 (m), 1195 (w), 1184 (w), 1155 (m), 1096 (m), 1080 (m), 1024 (m), 935 (m), 889 (w), 803 (m), 777 (m), 758 (m), 740 (m), 697 (m) cm^{-1}; elemental analysis (%) calcd for $C_{90}H_{136}K_2N_4Ni_2O_2S_2$ (1565.78 g mol^{-1}): C 69.04, H 8.75, N 3.58; found: C 69.31, H 8.84, N 3.99.

Reaction of (K·OEt_2)(K)[L^{tBu}Ni(SEt)]$_2$ (3) with CO. At r.t., an orange-red hexane suspension of (K·OEt_2)(K)[L^{tBu}Ni(SEt)]$_2$ (**3**) (27 mg, 19 μmol) was treated with excess CO and stirred for 15 min. The precipitation of a white solid was observed. Filtration of the suspension* and removal of all volatile materials afforded a red-brown solid of [L^{tBu}Ni(CO)] (10 mg, 17 μmol, 44%) as revealed by a ^{1}H NMR spectrum of a benzene-d_6 solution featuring two broad signals, which are characteristic for the nickel(I) carbonyl compound. ^{1}H NMR (300.1 MHz, C_6D_6): δ = 3.4 (br), 2.9 (br) ppm; IR (KBr): $\tilde{\nu}$ = 2009 (s, *CO*) cm^{-1}. *^{1}H NMR spectroscopy of a DMSO-d_6 solution of the remaining cruddy white residue proved the formation of KSEt. ^{1}H NMR (300.1 MHz, DMSO-d_6): δ = 2.21 (q, $^3J_{HH}$ = 7.3 Hz, 2H, $KSCH_2CH_3$), 1.04 (t, $^3J_{HH}$ = 7.3 Hz, 3H, $KSCH_2CH_3$) ppm.

Reaction of (K·OEt_2)$_2$[L^{tBu}Ni(SPh)]$_2$ (4) with CO. At r.t., an orange-red hexane solution of (K·OEt_2)$_2$[L^{tBu}Ni(SPh)]$_2$ (**4**) (39 mg, 25 μmol) was treated with excess CO and stirred for 10 min. The precipitation of a white solid was observed. All volatiles of the resulting red-brown suspension were removed in vacuum. The residue was extracted with hexane. Filtration* and removal of the solvent afforded a red-brown solid of [L^{tBu}Ni(CO)] (14 mg, 24 μmol, 48%) as revealed by a ^{1}H NMR spectrum of a benzene-d_6 solution featuring two broad signals, which are characteristic for the nickel(I) carbonyl compound. ^{1}H NMR (300.1 MHz, C_6D_6): δ = 3.4 (br), 2.9 (br) ppm; IR (KBr): $\tilde{\nu}$ = 2011 (s, *CO*) cm^{-1}. *^{1}H NMR spectroscopy of a DMSO-d_6 solution of the remaining cruddy white residue proved the formation of KSPh.

dx.doi.org/10.1021/ic500698v | *Inorg. Chem.* 2014, 53, 6867−6874

Table 3. X-ray Structure Parameters for the Nickel(II) and Nickel(I) Thiolate Complexes Discussed in This Work

	1	2	3	4
formula	$C_{37}H_{58}N_2NiS$	$C_{37}H_{59}N_3NiS$	$C_{78}H_{126}K_2N_4Ni_2OS_2$	$C_{90}H_{136}K_2N_4Ni_2O_2S_2$
fw	621.62	636.64	1395.57	1565.77
cryst syst	triclinic	monoclinic	orthorhombic	monoclinic
space group	$P\bar{1}$	Pc	$Pbcn$	$P2_1/n$
a /Å	9.6736(3)	10.4799(4)	26.4765(15)	12.7088(4)
b /Å	9.7346(3)	14.9728(5)	17.9487(10)	18.3156(6)
c /Å	41.7577(11)	11.5528(4)	16.7544(9)	19.4283(6)
α /deg	95.973(2)	90	90	90
β /deg	90.744(2)	107.423(3)	90	102.5970(10)
γ /deg	113.835(2)	90	90	90
V /Å^3	3570.81(18)	1729.62(11)	7962.0(8)	4413.5(2)
Z	4	2	4	2
calc density/g cm^{-3}	1.156	1.222	1.164	1.178
μ /mm^{-1}	0.628	0.650	2.329	0.615
F(000)	1352	692	3024	1692
θ /deg	2.30−26.60	3.29−27.90	2.97−66.73	2.42−28.34
reflections collected/unique	45 193/14 924 [R_{int} = 0.0931]	19 613/7951 [R_{int} = 0.0363]	58 562/7010 [R_{int} = 0.0508]	152 169/10 977 [R_{int} = 0.0631]
final R indices [$I > 2\sigma(I)$]	R_1 = 0.0436, wR_2 = 0.0908	R_1 = 0.0252, wR_2 = 0.0507	R_1 = 0.0355, wR_2 = 0.0837	R_1 = 0.0326, wR_2 = 0.1158
R indices (all data)	R_1 = 0.0773, wR_2 = 0.0963	R_1 = 0.0294, wR_2 = 0.0515	R_1 = 0.0542, wR_2 = 0.0925	R_1 = 0.0377, wR_2 = 0.1229
GOF	0.847	1.020	1.010	1.035

^{1}H NMR (300.1 MHz, DMSO-d_6): δ = 6.98 (d, $^3J_{HH}$ = 6.9 Hz, 2H, Ar-*o*H), 6.63 (t, $^3J_{HH}$ = 7.3 Hz, 2H, Ar-*m*H), 6.39 (t, $^3J_{HH}$ = 7.6 Hz, 1H, Ar-*p*H) ppm.

Crystal Structure Determinations. The data collections (see Table 3) were performed with a STOE IPDS 2T (**1** and **2**) or with a BRUKER D8 Venture (**3** and **4**) diffractometer at 100 K by using Mo Kα (**1**, **2**, **4**, λ = 0.710 73 Å) and Cu Kα (**3**, λ = 1.541 78 Å) radiation. The structures were solved by direct methods (SHELXS-97)[33] and refined by full-matrix least-squares procedures based on F^2 with all measured reflections (SHELXL-97,[34] SHELXL-2013[35]). All non-hydrogen atoms were refined anisotropically. All hydrogen atoms were added geometrically and refined by using a riding model. Additional crystallographic data, including CIF files, can be found in the Supporting Information.

■ ASSOCIATED CONTENT

Supporting Information

Additional spectroscopic data, ESI mass spectra, DFT calculations, and X-ray crystallographic data in cif format. This material is available free of charge via the Internet at http://pubs.acs.org. CCDC 984793 (**1**), CCDC 984794 (**2**), CCDC 984795 (**3**), and CCDC 984796 (**4**) contain the supplementary crystallographic data for this paper. These data can be obtained free of charge from The Cambridge Crystallographic Data Centre via www.ccdc.cam.ac.uk/data_request/cif.

■ AUTHOR INFORMATION

Corresponding Author

*E-mail: Christian.limberg@chemie.hu-berlin.de.

Notes

The authors declare no competing financial interest.

■ ACKNOWLEDGMENTS

We are grateful to the Cluster of Excellence "Unifying Concepts in Catalysis" funded by the Deutsche Forschungsgemeinschaft (DFG) as well as the Humboldt-Universität zu Berlin for financial support. Dr. S. Mebs is thanked for the X-ray analysis of **1**. We also thank C. Matlachowski and S. T. Li for EPR measurements.

■ REFERENCES

(1) Ragsdale, S. W. *J. Biol. Chem.* **2009**, *284*, 18571−18575.

(2) The existence of an additional sulfide ligand in a position bridging Ni and Fe$_d$, which was found in the crystal structure of CODH$_{Ch}$, led to controversy regarding the correct composition of the C-cluster and the catalytic role of the sulfide bridge. As this μ_2-S was not found in structures from CODH$_{Rr}$, CODH/ACS$_{Mt}$, or recombinant CODH$_{Ch}$ it may be concluded that the sulfide is absent in the catalytically active form of the C-cluster.[3,5,6]

(3) Kung, Y.; Doukov, T. I.; Seravalli, J.; Ragsdale, S. W.; Drennan, C. L. *Biochemistry* **2009**, *48*, 7432−7440.

(4) Appel, A. M.; Bercaw, J. E.; Bocarsly, A. B.; Dobbek, H.; DuBois, D. L.; Dupuis, M.; Ferry, J. G.; Fujita, E.; Hille, R.; Kenis, P. J. A.; Kerfeld, C. A.; Morris, R. H.; Peden, C. H. F.; Portis, A. R.; Ragsdale, S. W.; Rauchfuss, T. B.; Reek, J. N. H.; Seefeldt, L. C.; Thauer, R. K.; Waldrop, G. L. *Chem. Rev.* **2013**, *113*, 6621−6658.

(5) Kung, Y.; Drennan, C. L. *Curr. Opin. Chem. Biol.* **2011**, *15*, 276−283.

(6) Amara, P.; Mouesca, J.-M.; Volbeda, A.; Fontecilla-Camps, J. C. *Inorg. Chem.* **2011**, *50*, 1868−1878.

(7) Can, M.; Armstrong, F. A.; Ragsdale, S. W. *Chem. Rev.* **2014**, *114*, 4149−4174.

(8) (a) Ragsdale, S. W. *Chem. Rev.* **2006**, *106*, 3317−3337. (b) Bender, G.; Ragsdale, S. W. *Biochemistry* **2011**, *50*, 276−286.

(9) Bender, G.; Pierce, E.; Hill, J. A.; Darty, J. E.; Ragsdale, S. W. *Metallomics* **2011**, *3*, 797−815.

(10) The molecular structure of **I** is not listed in the Cambridge Structural Database, but the analogue complexes [L^{tBu}Ni(Cl)][11] and [L^{tBu}Ni(F)][12] are reported.

(11) Holland, P. L.; Cundari, T. R.; Perez, L. L.; Eckert, N. A.; Lachicotte, R. J. *J. Am. Chem. Soc.* **2002**, *124*, 14416−14424.

(12) Holze, P.; Horn, B.; Limberg, C.; Matlachowski, C.; Mebs, S. *Angew. Chem.* **2014**, *126*, 2788−2791; *Angew. Chem., Int. Ed.* **2014**, *53*, 2750−2753.

(13) For similar three-coordinate iron thiolates supported by the same bulky β-diketiminate ligand system, compare Chiang, K. P.; Barrett, P. M.; Ding, F.; Smith, J. M.; Kingsley, S.; Brennessel, W. W.; Clark, M. M.; Lachicotte, R. J.; Holland, P. L. *Inorg. Chem.* **2009**, *48*, 5106−5116.

(14) Evans, D. F. *J. Chem. Soc.* **1959**, 2003−2005.

(15) The resonance for the protons of the methyl group of the thiolate ligand (SCH_2CH_3) was also observed at δ(H) = 14 ppm. However, no signal for the methylene bridge (SCH_2CH_3) was detected, which may be due to its close proximity to the paramagnetic nickel center.

(16) For nickel(II) carbonyl complexes carrying thiolate ligands, see (a) Nguyen, D. H.; Hsu, H.-F.; Millar, M.; Koch, S. A.; Achim, C.; Bominaar, E. L.; Münck, E. *J. Am. Chem. Soc.* **1996**, *118*, 8963−8964. (b) Liaw, W.-F.; Chen, C.-H.; Lee, C.-M.; Lee, G.-H.; Peng, S.-M. *J. Chem. Soc., Dalton Trans.* **2001**, 138−143. (c) Ito, M.; Matsumoto, T.; Tatsumi, K. *Inorg. Chem.* **2009**, *48*, 2215−2223.
(17) Horn, B.; Pfirrmann, S.; Limberg, C.; Herwig, C.; Braun, B.; Mebs, S.; Metzinger, R. *Z. Anorg. Allg. Chem.* **2011**, *637*, 1169−1174.
(18) Horn, B.; Limberg, C.; Herwig, C.; Braun, B. *Chem. Commun.* **2013**, *49*, 10923−10925.
(19) Pulukkody, R.; Kyran, S. J.; Bethel, R. D.; Hsieh, C.-H.; Hall, M. B.; Darensbourg, D. J.; Darensbourg, M. Y. *J. Am. Chem. Soc.* **2013**, *135*, 8423−8430.
(20) Tian, X.; Goddard, R.; Pörschke, K.-R. *Organometallics* **2006**, *25*, 5854−5862.
(21) Räke, B.; Zülch, F.; Ding, Y.; Prust, J.; Roesky, H. W.; Noltemeyer, M.; Schmidt, H.-G. *Z. Anorg. Allg. Chem.* **2001**, *627*, 836−840.
(22) Decomposition processes start immediately after dissolution of isolated **2**.
(23) Pfirrmann, S.; Limberg, C.; Herwig, C.; Knispel, C.; Braun, B.; Bill, E.; Stösser, R. *J. Am. Chem. Soc.* **2010**, *132*, 13684−13691.
(24) Desrochers, P. J.; Cutts, R. W.; Rice, P. K.; Golden, M. L.; Graham, J. B.; Barclay, T. M.; Cordes, A. W. *Inorg. Chem.* **1999**, *38*, 5690−5694.
(25) For example, see (a) Buonomo, R. M.; Font, I.; Maguire, M. J.; Reibenspies, J. H.; Tuntulani, T.; Darensbourg, M. Y. *J. Am. Chem. Soc.* **1995**, *117*, 963−973. (b) Hosler, E. R.; Herbst, R. W.; Maroney, M. J.; Chohan, B. S. *Dalton Trans.* **2012**, *41*, 804−816.
(26) Gehring, H.; Metzinger, R.; Herwig, C.; Intemann, J.; Harder, S.; Limberg, C. *Chem.—Eur. J.* **2013**, *19*, 1629−1636.
(27) Beck, R.; Shoshani, M.; Krasinkiewicz, J.; Hatnean, J. A.; Johnson, S. A. *Dalton Trans.* **2013**, *42*, 1461−1475.
(28) Gennari, M.; Orio, M.; Pécaut, J.; Bothe, E.; Neese, F.; Collomb, M.-N.; Duboc, C. *Inorg. Chem.* **2011**, *50*, 3707−3716.
(29) The product of the reduction was only sparingly soluble in hexane. Therefore, it was extracted with diethyl ether, and the solvent was removed to give a red solid of **3**.
(30) Bai, G.; Wei, P.; Stephan, D. W. *Organometallics* **2005**, *24*, 5901−5908.
(31) In hexane solutions of **4** (as well as in toluene solutions of **3**) the *g* anisotropy is almost eliminated.
(32) Pfirrmann, S.; Limberg, C.; Herwig, C.; Stößer, R.; Ziemer, B. *Angew. Chem.* **2009**, *121*, 3407−3411; *Angew. Chem., Int. Ed.* **2009**, *48*, 3357−3361.
(33) Sheldrick, G. M. *SHELXS-97, Program for Crystal Structure Solution;* University of Göttingen: Göttingen, Germany, 1997.
(34) Sheldrick, G. M. *SHELXL-97, Program for Crystal Structure Refinement;* University of Göttingen: Göttingen, Germany, 1997.
(35) Sheldrick, G. M. *SHELXL-2013, Program for Crystal Structure Refinement;* University of Göttingen: Göttingen, Germany, 2013.